



Cite this: *RSC Adv.*, 2017, 7, 24163

[2 + 2 + 2] cyclotrimerisation as a convenient route to 6N-doped nanographenes: a synthetic introduction to hexaazasuperbenzenes†‡

Lankani P. Wijesinghe,^a Sarath D. Perera,^{ab} Eugene Larkin,^a Gearóid M. Ó Máille,^a Robert Conway-Kenny,^a Buddhie S. Lankage,^a Longsheng Wang^a and Sylvia M. Draper^{*a}

Received 3rd March 2017
 Accepted 21st April 2017

DOI: 10.1039/c7ra02648j

rsc.li/rsc-advances

6N-containing polyphenylene precursors were generated *via* [2 + 2 + 2] cyclotrimerisation. On methoxy substitution complete ring-closure can be achieved (*via* FeCl₃-mediated oxidative cyclodehydrogenation) to give asymmetric and C_{3v} symmetric hexaazasuperbenzenes. Investigations using DDQ/H⁺ mediated conditions reveal this to be a promising alternative and selective route to partial cyclodehydrogenation.

It is now well-documented that the incorporation of heteroatoms such as N,^{1–3} P,^{4,5} S,^{6–8} or B^{9,10} into the core of polycyclic aromatic hydrocarbon (PAH) derivatives fundamentally affects their electronic and optical properties.^{11–13} It is one means by which to tailor the HOMO–LUMO gap in such materials and to confer upon them either p- or n-type semiconducting properties as required in organic field-effect transistors and organic light emitting diodes.^{14–16} Depending on the position of the heteroatom (periphery or core), such substituents can also provide ligand or coordination functionality to PAH-based molecules.^{17,18} This latter effect has been demonstrated most notably in systems with a coronene skeleton as part of their aromatic core and pyrimidine units in peripheral sites.^{19,20} The introduction of graphitic nitrogen atoms also opens up the possibility of new applications *e.g.* as sites for enhancing the electrocatalytic behaviour of carbon-materials.²¹

Polycyclic heteroaromatics based on hexaphenylbenzene have emerged as desirable synthetic targets on many fronts, not just as a starting unit for bottom-up synthesis but also as well-defined substructures for the surface-mediated formation of heteroatom-doped graphene and nanoribbons.^{11,22,23} However, the synthetic challenges are magnified by the presence of these heteroatoms, and have led to interesting strategies that differ significantly from their all-carbon analogues.²⁴ In terms of

controlling the nature and extent of heteroatom doping, there is still much to achieve in the resulting substitution patterns and the degree of ring fusion. In unfused systems, 6N substitution of hexaphenylbenzene has recently been achieved.²⁵ Fused 2N and 4N systems have been generated through the use of pyrimidyl units,²⁶ while 6N substitution has only been achieved in pyrrole-based systems.³

This work aims to tackle one of the current major challenges, that of increasing the degree of N-doping into the periphery of the aromatic core without compromising the extent of aromaticity in the final product. In the process we have produced hexaazasuperbenzenes with differing anisotropic molecular shapes, structural rigidity, extended π-surfaces, and shed some light on how N-doping influences the outcome of metal and DDQ/H⁺ mediated cyclodehydrogenation reactions.

[2 + 2 + 2] cycloadditions involving alkynes have been used as an elegant, one-step and potentially one-reagent method for the generation of annulated benzene derivatives.²⁷ Herein, we exploit the [2 + 2 + 2] trimerisation of pyrimidyl containing acetylenes as a convenient route to yield 6N-doped polyphenylenes in high yield. The subsequent oxidative cyclodehydrogenation reactions gave nitrogen-doped nanographenes with N-loadings of up to 11.11 atom% within the aromatic core with differing N-donor arrangements.

Two series of 6N polyphenylenes were synthesised by varying the functional groups in the monopyrimidyl acetylene precursor (*tert*-butyl or methoxy – see Schemes 1 and 2) and subjecting them to standard dicobalt octacarbonyl-catalysed cyclotrimerisation conditions.²⁸ Asymmetric 3,5,6-tri-(4-*tert*-butylphenyl)-1,2,4-tri(5-pyrimidyl)benzene (**1**), and the symmetric 2,4,6-tri(4-*tert*-butylphenyl)-1,3,5-tri(5-pyrimidyl)benzene (**2**) (Scheme 1), were successfully isolated as white crystalline solids in 68% and 27% yields respectively, in the expected statistical ratio of 3 : 1 [see ESI

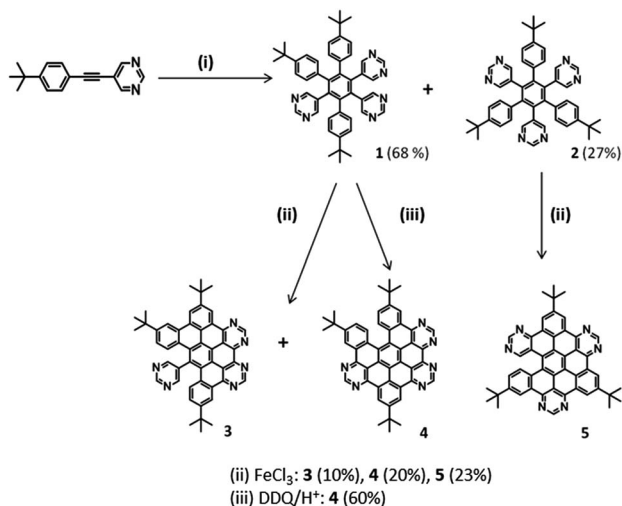
^aSchool of Chemistry, Trinity College, Dublin, D2, Ireland. E-mail: smdraper@tcd.ie

^bChemistry Department, Open University of Sri Lanka, Nugegoda, Sri Lanka

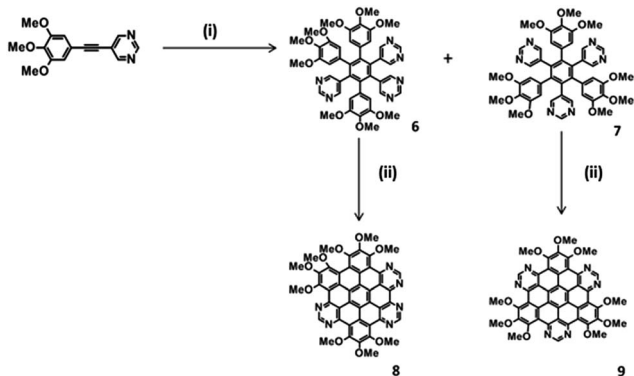
† The work was supported financially by Science Foundation Ireland (SFI/IA/3046, SFI/09/IN.1/12974), and Trinity postgraduate awards.

‡ Electronic supplementary information (ESI) available: all experimental procedures, ¹H/¹³C NMR, HRMS, UV-Vis (absorption and emission) for nanographenes 3–5 and 8. Cyclic voltammograms for 3–5. Single crystal X-ray data for 2. CCDC 1507271. For ESI and crystallographic data in CIF or other electronic format see DOI: 10.1039/c7ra02648j





Scheme 1 Synthetic route to *tert*-butyl functionalised 6N-doped hexaazasuperbenzenes (HASB): (i) $\text{Co}_2(\text{CO})_8$, dioxane, 115 °C, 24 h, under N_2 , (ii) FeCl_3 , CH_3NO_2 , CH_2Cl_2 , 298 K, Ar bubbling, 72 h, (iii) DDQ, MeSO_3H or $\text{CF}_3\text{SO}_3\text{H}$, CH_2Cl_2 .



Scheme 2 Synthetic route to methoxy-functionalised hexaazasuperbenzenes (HASB). (i) $\text{Co}_2(\text{CO})_8$, dioxane, 115 °C, 24 h, under N_2 , (ii) FeCl_3 , CH_3NO_2 , CH_2Cl_2 , 298 K, Ar bubbling, 24 h.

for single crystal X-ray structure of **2** (S5†) and the photophysical investigation of **1** and **2** (S6a†)]. These materials are isomers, differing in terms of their symmetry patterns (C_{3v} or star-shaped, and asymmetric).

The planarisation of the *tert*-butyl functionalised 6N polyphenylenes **1** and **2** to obtain 6N nanographenes was studied under a range of common oxidative cyclodehydrogenation conditions: (i) $\text{AlCl}_3/\text{CuCl}_2/\text{CS}_2$ (ii) $\text{FeCl}_3/\text{CH}_3\text{NO}_2/\text{CH}_2\text{Cl}_2$ and (iii) DDQ/H^+ (where $\text{H}^+ = \text{MeSO}_3\text{H}$ or $\text{CF}_3\text{SO}_3\text{H}$). For the asymmetric polyphenylene **1**, the $\text{AlCl}_3/\text{CuCl}_2/\text{CS}_2$ route resulted in a myriad of partially fused products. Although the separation of these was extremely challenging, 5/6th fused (five C–C bonds closed) **4** was isolated in very low yield (5%) after a series of purification attempts.

By comparison, the FeCl_3 -catalysed procedure proved to be much cleaner: the oxidative cyclodehydrogenation of asymmetric **1** under FeCl_3 -mediated conditions resulted in the 2/3rd-fused (four C–C bonds formed) **3** and 5/6th fused (five C–C bonds

formed) **4** as the two major products (Scheme 1). Preparative thin layer chromatography facilitated the separation of these co-synthesised products **3** (10%) and **4** (20%). In addition, mass spectrometric analysis of the crude mixture showed the presence of 1/2-fused (three C–C bonds formed) and 1/3rd fused (two C–C bonds formed) compounds in trace amounts [see S4(a)†]. Under the same FeCl_3 -conditions, the oxidative cyclodehydrogenation of symmetric **2** resulted in the 5/6th fused (five C–C bonds formed) **5** (23%) as the major product. As for **1**, the mass spectrometric analysis of the crude reaction material showed the presence of other partially-fused products with varying degrees of fusion [S4(b)†]. For symmetric **2**, the AlCl_3 route was not successful and resulted in a mixture of intractable products.

Recently, ring closure *via* DDQ/H^+ oxidation has been explored as a metal-free alternative for the oxidative cyclodehydrogenation of various all-carbon aromatic donors.²⁹ To the best of our knowledge, this route has not been tested for N-containing polyphenylene systems. In this work, the DDQ/H^+ -mediated oxidative cyclodehydrogenation was investigated for 6N polyphenylene **1**, resulting in 5/6th fused **4** as the major product in 60% yield. Since the DDQ/H^+ route did not result in other partially fused products, 5/6th fused **4** was isolated in good yield and the purification was relatively straightforward. Interestingly, the five C–C bond closures have taken place at the same positions as in the 5/6th fused product obtained *via* FeCl_3 and AlCl_3 (as confirmed by NMR analysis, see S3†). Furthermore, with extended reaction times (up to 5 days) and the excess addition of FeCl_3 (60 equivalents), we were unable to obtain complete ring closure in either *tert*-butyl functionalised asymmetric **1** or symmetric **2**. Given recent literature reports of the efficacy of using stronger acids in the DDQ/H^+ process particularly in electron poor polyphenylenes,³⁰ the authors modified their reaction conditions to determine if $\text{CF}_3\text{SO}_3\text{H}$ would improve the outcome of the reaction. No change was seen either in the nature of the products arising or the yield of **4** produced.

A second series of methoxy-functionalised 6N polyphenylenes was synthesised *via* cobalt mediated cyclotrimerisation using 5-(3,4,5-trimethoxyphenylethynyl)pyrimidine as the precursor (Scheme 2). The methoxy groups were incorporated to increase the efficiency of the subsequent oxidative cyclodehydrogenation step.³¹ Both asymmetric 3,5,6-tri-(3,4,5-trimethoxyphenyl)-1,2,4-tri-(5-pyrimidyl)benzene (**6**) and symmetric 2,4,6-tri-(3,4,5-trimethoxyphenyl)-1,3,5-tri-(5-pyrimidyl)benzene (**7**) were successfully isolated *via* column chromatography in 63% and 17% yields respectively (Scheme 2).

Oxidative cyclodehydrogenation of methoxy-substituted asymmetric **6** under FeCl_3 -mediated oxidative cyclodehydrogenation resulted in fully fused (six C–C bonds formed) **8**. Preliminary mass spectral analysis of the crude material indicated the presence of a mixture of products [see S4(c)†], showing the presence of the fully-fused product **8**, along with a 5/6th fused product (five C–C bonds formed). Preparative plate chromatography (SiO_2) using toluene : methanol (20 : 1) as eluent proved to give the best separation. The isolated yield of the pure fully-fused product **8** was low (10%) due to the challenges faced in purification, however **8** is the first example of a fully-fused hexaazasuperbenzene (HASB). Under FeCl_3 mediated oxidative cyclodehydrogenation, symmetric



7, resulted in the fully-fused and 5/6th fused compounds according to mass spectrometric evidence of the crude [see S4(d)†]. In this case the two products could not be separated despite attempting various purification methods.

Fig. 1a compares the absorption spectra of compounds **3**, **4**, **5** and **8** along with a 4N tetraaza reference compound (**N-HSB**) in toluene. **4** and **5**, with similar degrees of aromaticity, show similar structural features in their absorption spectra, e.g. $\lambda_{\text{max}}^{\text{abs}} = 325$ nm. In comparison the 2/3rd-fused **3** shows a slightly hypsochromically shifted spectrum, due to the decrease in size of its aromatic platform. The methoxy HASB **8** shows the typical structured UV-Vis absorption spectrum of a rigid, fully-fused system centred around $\lambda_{\text{max}}^{\text{abs}} = 365$ nm.

Methoxy functionalisation has bathochromically shifted the λ_{max} absorption compared to all carbon HBC³² and **N-HSB** (Fig. 1), which typically show an absorption maxima band at λ_{max} 355 nm. This band is characteristic of the β band described by Clar,³³ which is generally $\pi-\pi^*$ in character with some $n-\pi^*$ character for N-containing systems. In comparison to the reference **N-HSB** molecule, the electron-donating methoxy substituents in **8** destabilise the HOMO to a greater extent while the increased N content stabilises the LUMO. A combination of both these effects results in a reduced HOMO-LUMO gap, and the relatively red-shifted absorption spectrum of **8** compared to **N-HSB** (Fig. 1a). This gap can be calculated directly using the α -band position of the compounds, revealing that the gap is smaller for **8** (2.52 eV) than **N-HSB**¹ (2.58 eV) and its methoxy-substituted diaza (2N) analogue (2.61 eV).³¹

The overlaid emission spectra of HASBs **3**, **4**, **5** and **8** along with reference compound **N-HSB** are shown in Fig. 1b. A comparison of the spectra of 5/6th fused **4** and **5** shows that they have similar spectral shapes, with $\lambda_{\text{max}}^{\text{em}} = 495$ nm. The 2/3rd-fused **3** exhibits a relatively blue-shifted spectrum in comparison,

with $\lambda_{\text{max}}^{\text{em}} = 463$ nm and a second band appearing at $\lambda = 495$ nm, due to its reduced aromaticity. It is interesting to note that the emission spectra of the 5/6th-fused products resembles that of **N-HSB**, with a common $\lambda_{\text{max}}^{\text{em}} = 494$ nm in toluene. Furthermore, comparing diaza³¹ (2N) and the all carbon analogue HBC,³² a trend is apparent that upon increasing the number of the N-dopants in the platform, the vibronic structure observed in the emission is lost. This is mainly due to the availability of hydrogen bonding sites on the molecule.

Solvent dependency studies are a useful tool to investigate the nature of the electronic transitions in absorption and emission spectra. The solvent dependent absorption studies of **4** (Fig. 2a) show a bathochromic shift along with a slight broadening of the lower energy bands on increasing the polarity of the solvent. The corresponding solvent dependent emission study is presented in Fig. 2b. The compound is intensely fluorescent, and exhibits prominent vibrational progressions in non-polar solvents (e.g. hexane). As the solvent polarity increases, the vibronic progression is lost and a broad emission results, particularly in methanol. There is a significant bathochromic shift of the λ_{max} (~ 2900 cm^{-1}) in going from hexane to methanol. This agrees with the assignment of the first excited state S_1 as having $^1(\pi-\pi^*)$ character.³⁴ The enhanced interaction of the more polar solvent molecules with the chromophore in its excited state (often *via* H-bond formation), lowers its excited state energy and shifts the emission to longer wavelengths.

The 6N methoxy substituted **8** shows a broad emission with $\lambda_{\text{max}}^{\text{em}} = 515$ nm and is further red-shifted compared to its *tert*-butyl counterparts (**3**, **4** and **5**) (see Fig. 1b). Both the inclusion of electron-donating methoxy substituents and the increase in conjugation contribute to the red-shift in emission observed in **8**. All of the HASB systems showed comparable lifetimes in the ns range (4–8 ns) at room temperature (Table 1). These

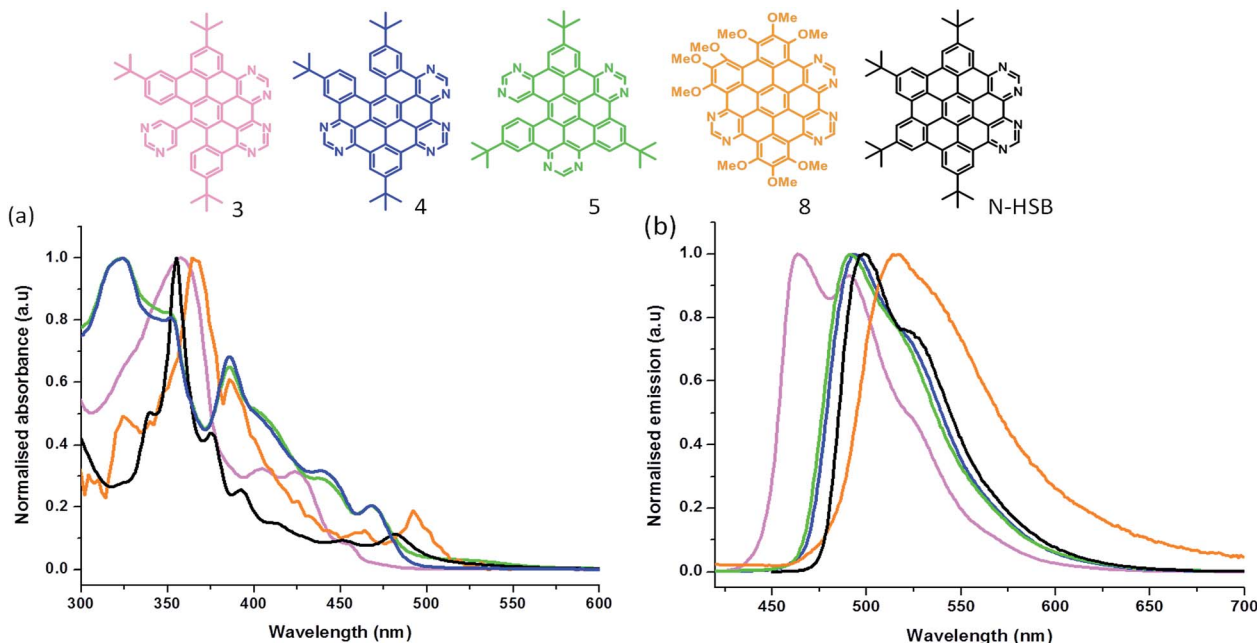


Fig. 1 Normalised (a) UV-Visible absorption spectra and (b) emission spectra of **3**, **4**, **5**, **8** and **N-HSB** ($\lambda_{\text{exc}} = 360$ nm, $\sim 10^{-6}$ M) in toluene.



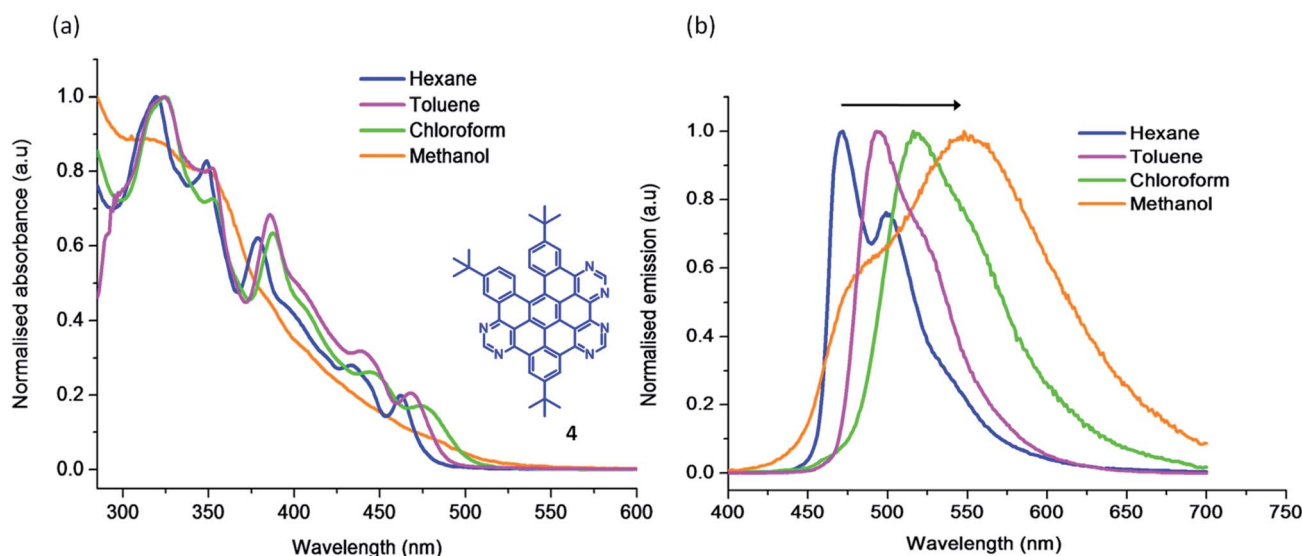


Fig. 2 The (a) absorption and (b) emission spectra of **4** in the indicated solvents ($\sim 10^{-6}$ M) at RT.

nanosecond scale lifetimes further confirm that the emission is mainly from the $^1(\pi-\pi^*)$ excited state. **4** displays an emission quantum yield of $\Phi_{em} = 0.3$ in CHCl_3 . This slightly reduced quantum yield relative to **N-HSB** ($\Phi_{em} = 0.4$ in toluene) may be a feature of its reduced planarity offering a mechanism to deactivate its excited state *via* non-radiative pathways.

Cyclic voltammetric studies were carried out in dry, degassed dichloromethane using a glassy carbon working electrode (Table 1 and S7 \ddagger). **4** shows an irreversible oxidation wave at $E_{pa} = +1.25$ V, however the symmetric analogue **5** shows no clear oxidation potential within the spectral window analysed (see S7 in ESI \ddagger). The 2/3-fused **3** ($E_{pa} = +1.3$ V) showed a slightly higher oxidation potential compared to its 5/6th-fused counterpart **4**. The reduced aromaticity in **3** gives rise to a stabilized HOMO making the oxidation in **3** slightly more difficult than **4**. The low yields obtained for **8** prevented electrochemical measurements. From the extrapolation of data from previous 2N³¹ and 4N systems synthesised by Draper *et al.*, the degree of difficulty in

oxidation increases with an increasing number of N-dopants. This is due to the reduced electron density in the aromatic platform, leading to stabilisation of the HOMO. As a result, the oxidation of the 6N systems was far more difficult compared to their all-carbon, 2N or 4N counterparts.

The reduction potentials are mainly governed by the electron withdrawing N-atoms present (Table 1 and S7 \ddagger). Compound **4** shows three reversible reductions at $E_{1/2} = -1.57$ V, -1.94 V and -2.32 with **5** showing similar reduction behaviour ($E_{1/2} = -1.55$ V, -1.91 V, -2.19 V). The reduction processes of **5** occur in a broader window than those of **4** which shows a set of clear sharp reduction waves. This supports the observation that **5** undergoes stacking in solution at higher concentrations. The reduction potentials of the 6N systems show that they are more readily reduced compared to the all-carbon, 2N or 4N systems. This is consistent with the increasing electron accepting character of the molecules as a function of the pyrimidyl N-atoms and the stabilisation of the LUMO.

Table 1 UV-Visible absorption, emission spectral data in toluene (RT, $\sim 10^{-6}$ M) and electrochemical data in CH_2Cl_2 (0.1 M, $^n\text{Bu}_4\text{NPF}_6$) for **3**, **4**, **5**, **8** and THF for **N-HSB** at 298 K

Compound	λ_{abs} [nm] ($\epsilon \times 10^4$) [$\text{M}^{-1} \text{cm}^{-1}$]	λ_{em} [nm] (λ_{exc} [nm])	τ /ns (λ_{exc} [nm]) (λ_{nm})	Oxidation $E_{1/2}/\text{V}$ [ΔE_p mV]	Reduction $E_{1/2}/\text{V}$ [ΔE_p mV]
3	295(1.8), 357(5.0), 405(2.1), 423(2.0), 455(0.8)	463 _{max} , 495 (360)	7.8(295/463)	+1.3 ^a	-1.56[55], -1.88[59], -2.18[91]
4	323(11.3), 352(9.2), 385(7.8), 440(3.5), 468(2.2)	495(360)	6.9(340/495)	+1.25 ^a	-1.57[48], -1.91[43], -2.19[45]
5	323(11.0), 352(9.1), 385(7.6), 440(3.3), 468(2.1)	495(360)	5.3(340/495)	No oxidation ^b	-1.55[48], -1.91[43], -2.19[45]
8	325(6.0), 365(12.1), 386(8.1), 462(2.9), 492(3.3)	514(360)	4.6(340/514)	—	—
NHSB	339(5.7), 355(13.7), 376(5.4), 393(3.2), 413(1.5), 451(1.0), 481(1.4)	494 _{max} , 524 _{sh} (360)	13(340/494)	+0.9 ^a	-1.56[60], -2.00[102], -2.32 ^a

^a Process is irreversible. ^b No oxidation in potential window analysed.



In summary, cobalt octacarbonyl-catalysed [2 + 2 + 2] cyclo-trimerisations proved a convenient route to synthesise four 6N containing polyphenylene precursors. The two *tert*-butyl functionalised 6N polyphenylenes undergo oxidative cyclo-dehydrogenation using various oxidants to give partially fused systems. The incorporation of methoxy functional groups onto the polyphenylene precursors however facilitates complete ring closure *via* FeCl₃. Cyclo-dehydrogenation using DDQ/H⁺ was demonstrated as a promising metal-free alternative route for aromatisation of N-containing polyphenylene systems. It gives rise to significantly increased yields and selectivity of ring closure irrespective of the strength of the acid used. Pending the development of appropriate ring-closure conditions, this cyclo-trimerisation approach could be used to access nanographenes with a possible N-loading of 25 atom%. The novel molecular systems generated in this work offer a new opportunity to investigate the influence of N-doping patterns on the supramolecular architectures of the molecules themselves and the nature and properties of their coordination complexes.

Acknowledgements

We thank Drs J. O'Brien, M. Ruether and M. Feeney for spectroscopic and technical assistance.

Notes and references

- 1 S. M. Draper, D. J. Gregg and R. Madathil, *J. Am. Chem. Soc.*, 2002, **124**, 3486–3487.
- 2 A. Graczyk, F. A. Murphy, D. Nolan, V. Fernandez-Moreira, N. J. Lundin, C. M. Fitchett and S. M. Draper, *Dalton Trans.*, 2012, **41**, 7746–7754.
- 3 M. Takase, V. Enkelmann, D. Sebastiani, M. Baumgarten and K. Müllen, *Angew. Chem., Int. Ed.*, 2007, **46**, 5524–5527.
- 4 P.-A. Bouit, A. Escande, R. Szűcs, D. Szieberth, C. Lescop, L. Nyulászi, M. Hissler and R. Réau, *J. Am. Chem. Soc.*, 2012, **134**, 6524–6527.
- 5 T. Baumgartner, *Acc. Chem. Res.*, 2014, **47**, 1613–1622.
- 6 C. J. Martin, B. Gil, S. D. Perera and S. M. Draper, *Chem. Commun.*, 2011, **47**, 3616–3618.
- 7 Y.-Z. Tan, S. Osella, Y. Liu, B. Yang, D. Beljonne, X. Feng and K. Müllen, *Angew. Chem., Int. Ed.*, 2015, **54**, 2927–2931.
- 8 L. Chen, S. R. Puniredd, Y.-Z. Tan, M. Baumgarten, U. Zschieschang, V. Enkelmann, W. Pisula, X. Feng, H. Klauk and K. Müllen, *J. Am. Chem. Soc.*, 2012, **134**, 17869–17872.
- 9 C. Dou, S. Saito, K. Matsuo, I. Hisaki and S. Yamaguchi, *Angew. Chem., Int. Ed.*, 2012, **51**, 12206–12210.
- 10 F. Miyamoto, S. Nakatsuka, K. Yamada, K.-i. Nakayama and T. Hatakeyama, *Org. Lett.*, 2015, **17**, 6158–6161.
- 11 M. Stepień, E. Gońka, M. Żyła and N. Sprutta, *Chem. Rev.*, 2017, **117**, 3479–3716.
- 12 M. Fan, Z.-Q. Feng, C. Zhu, X. Chen, C. Chen, J. Yang and D. Sun, *J. Mater. Sci.*, 2016, **51**, 10323–10349.
- 13 J. Duan, S. Chen, M. Jaroniec and S. Z. Qiao, *ACS Catal.*, 2015, **5**, 5207–5234.
- 14 W. Delaunay, R. Szűcs, S. Pascal, A. Mocanu, P. A. Bouit, L. Nyulaszi and M. Hissler, *Dalton Trans.*, 2016, **45**, 1896–1903.
- 15 J. Wu, W. Pisula and K. Müllen, *Chem. Rev.*, 2007, **107**, 718–747.
- 16 M. Oehzelt, C. Laubschat and D. V. Vyalikh, *Nano Lett.*, 2011, **11**, 5401–5407.
- 17 D. Nolan, B. Gil, F. A. Murphy and S. M. Draper, *Eur. J. Inorg. Chem.*, 2011, **2011**, 3248–3256.
- 18 F. A. Murphy and S. M. Draper, *J. Org. Chem.*, 2010, **75**, 1862–1870.
- 19 S. M. Draper, D. J. Gregg, E. R. Schofield, W. R. Browne, M. Duati, J. G. Vos and P. Passaniti, *J. Am. Chem. Soc.*, 2004, **126**, 8694–8701.
- 20 D. J. Gregg, E. Bothe, P. Höfer, P. Passaniti and S. M. Draper, *Inorg. Chem.*, 2005, **44**, 5654–5660.
- 21 H. Wang, T. Maiyalagan and X. Wang, *ACS Catal.*, 2012, **2**, 781–794.
- 22 A. L. Pinardi, J. I. Martinez, A. Jancarik, I. G. Stara, I. Stary, M. F. Lopez, J. Mendez and J. A. Martin-Gago, *Chem. Commun.*, 2014, **50**, 1555–1557.
- 23 L. Chen, Y. Hernandez, X. Feng and K. Müllen, *Angew. Chem., Int. Ed.*, 2012, **51**, 7640–7654.
- 24 A. Narita, X.-Y. Wang, X. Feng and K. Müllen, *Chem. Soc. Rev.*, 2015, **44**, 6616–6643.
- 25 Y. Xiang, Q. Wang, G. Wang, X. Li, D. Zhang and W. Jin, *Tetrahedron*, 2016, **72**, 2574–2580.
- 26 C. Delaney, G. M. Ó. Máille, B. Twamley and S. M. Draper, *Org. Lett.*, 2016, **18**, 88–91.
- 27 C. D. Simpson, J. Wu, M. D. Watson and K. Müllen, *J. Mater. Chem.*, 2004, **14**, 494–504.
- 28 X. Feng, W. Pisula, T. Kudernac, D. Wu, L. Zhi, F. S. De and K. Müllen, *J. Am. Chem. Soc.*, 2009, **131**, 4439–4448.
- 29 L. Zhai, R. Shukla and R. Rathore, *Org. Lett.*, 2009, **11**, 3474–3477.
- 30 D. J. Jones, B. Purushothaman, S. Ji, A. B. Holmes and W. W. H. Wong, *Chem. Commun.*, 2012, **48**, 8066–8068.
- 31 L. P. Wijesinghe, B. S. Lankage, G. M. O. Maille, S. D. Perera, D. Nolan, L. Wang and S. M. Draper, *Chem. Commun.*, 2014, **50**, 10637–10640.
- 32 W. Hendel, Z. H. Khan and W. Schmidt, *Tetrahedron*, 1986, **42**, 1127–1134.
- 33 E. Clar, *Polycyclic Hydrocarbons*, Academic Press, 1964, vol. 2.
- 34 R. P. Wayne, *Photochemistry*, Elsevier, 1971.

